Electrodynamics, Microwave Engineering, Antennas

УДК 621.372.833 Original article

https://doi.org/10.32603/1993-8985-2019-22-5-17-32

# Wideband Waveguide-to-Microstrip Transition for mm-Wave Applications

**Andrey V. Mozharovskiy[1]✉, Oleg V. Soykin[1], Aleksey A. Artemenko[1], Roman O. Maslennikov[1], Irina B. Vendik[2]**

[1]LLC "Radio Gigabit", Nizhny Novgorod, Russia

[2]Saint Petersburg Electrotechnical University, Saint Petersburg, Russia

✉andrey.mozharovskiy@radiogigabit.com

**Abstract**

**Introduction.** Increased data rate in modern communication systems can be achieved by raising the operational frequency to millimeter wave range where wide transmission bands are available. In millimeter wave communication systems, the passive components of the antenna feeding system, which are based on hollow metal waveguides, and active elements of the radiofrequency circuit, which have an interface constructed on planar printed circuit boards (PCB) are interconnected using waveguide-to-microstrip transition.

**Aim.** To design and investigate a high-performance wideband and low loss waveguide-to-microstrip transition dedicated to the 60 GHz frequency range applications that can provide effective transmission of signals between the active components of the radiofrequency circuit and the passive components of the antenna feeding system

**Materials and methods.** Full-wave electromagnetic simulations in the CST Microwave Studio software were used to estimate the impact of the substrate material and metal foil on the characteristics of printed structures and to calculate the waveguide-to-microstrip transition characteristics. The results were confirmed via experimental investigation of fabricated wideband transition samples using a vector network analyzer

**Results.** The probe-type transition consists of a PCB fixed between a standard WR-15 waveguide and a back-short with a simple structure and the same cross-section. The proposed transition also includes two through-holes on the PCB in the center of the transition area on either side of the probe. A significant part of the lossy PCB dielectric is removed from that area, thus providing wideband and low-loss performance of the transition without any additional matching elements. The design of the transition was adapted for implementation on the PCBs made of two popular dielectric materials RO4350B and RT/Duroid 5880. The results of full-wave simulation and experimental investigation of the designed waveguide to microstrip transition are presented. The transmission bandwidth for reflection coefficient $S_{11}$ < –10 dB is in excess of 50...70 GHz. The measured insertion loss for a single transition is 0.4 dB and 0.7 dB relatively for transitions based on RO4350B and RT/Duroid 5880.

**Conclusion.** The proposed method of insertion loss reduction in the waveguide-to-microstrip transition provides effective operation due to decrease of the dielectric substrate portion in the transition region for various high-frequency PCB materials. The designed waveguide-to -microstrip transition can be considered as an effective solution for interconnection between the waveguide and microstrip elements of the various millimeter-wave devices dedicated for the 60 GHz frequency range applications.

**Key words**: millimeter-wave band; waveguide-to-microstrip transition; printed circuit board; metal waveguide

**For citation:** Mozharovskiy A. V., Soykin O. V., Artemenko A. A., Maslennikov R. O., Vendik I. B. Wideband Waveguide-to-Microstrip Transition for mm-Wave Applications. Journal of the Russian Universities. Radioelectronics. 2019, vol. 22, no. 5, pp. 17–32. doi: 10.32603/1993-8985-2019-22-5-17-32

**Conflict of interest.** Authors declare no conflict of interest.

Submitted 27.03.2019; accepted 16.08.2019; published online 29.11.2019

Известия вузов России. Радиоэлектроника. 2019. Т. 22, № 5. С. 17–32
Journal of the Russian Universities. Radioelectronics. 2019, vol. 22, no. 5, pp. 17–32

Электродинамика, микроволновая техника, антенны

Оригинальная статья

# Широкополосный волноводно-микрополосковый переход зондового типа миллиметрового диапазона длин волн

**А. В. Можаровский[1]✉, О. В. Сойкин[1], А. А. Артеменко[1], Р. О. Масленников[1], И. Б. Вендик[2]**

[1]ООО "Радио Гигабит", Нижний Новгород, Россия

[2]Санкт-Петербургский государственный электротехнический университет "ЛЭТИ" им. В. И. Ульянова (Ленина), Санкт-Петербург, Россия

✉ andrey.mozharovskiy@radiogigabit.com

**Аннотация**

**Введение.** Для увеличения скорости передачи данных в современных системах беспроводной радиосвязи необходимо существенное расширение полосы частот передаваемых сигналов, что возможно за счет увеличения рабочей частоты до миллиметрового диапазона. В системах радиосвязи миллиметрового диапазона соединение пассивных элементов антенно-фидерного тракта, реализованных на металлических волноводах, и активных элементов радиочастотного тракта, имеющих интерфейс на основе микрополосковых линий, осуществляется с помощью волноводно-микрополоскового перехода (ВМПП).

**Цель работы.** Разработка и исследование широкополосного ВМПП для частотного диапазона 60 ГГц с низким уровнем потерь для эффективной передачи сигналов между активными элементами радиочастотного тракта и пассивными элементами антенного тракта.

**Материалы и методы.** Оценка влияния материала подложки и свойств металлической фольги на характеристики печатных структур и расчет характеристик разработанного перехода выполнены с помощью электродинамического моделирования в системе автоматизированного проектирования CST Microwave Studio и подтверждены результатами экспериментального исследования изготовленных образцов широкополосного волноводно-микрополоскового перехода на векторном анализаторе цепей.

**Результаты.** Разработанный ВМПП основан на использовании проводящего зонда, реализованного на печатной плате, закрепленной между стандартным подводящим волноводом WR15 и четвертьволновой заглушкой того же сечения. Для уменьшения потерь в переходе на печатной плате выполнены сквозные неметаллизированные отверстия, симметрично расположенные вокруг зонда для уменьшения доли диэлектрика печатной платы в волноводном канале. По результатам экспериментального исследования изготовленных макетов переходов, реализованных на печатных платах, выполненных из материалов RO4350B и RT/Duroid 5880 производства компании "Rogers", было получено, что переход согласован по уровню коэффициента отражения $S_{11} < -10$ дБ в полосе частот 50...70 ГГц и обеспечивает потери на прохождение не более 0.4 и 0.7 дБ для материалов RT/Duroid 5880 и RO4350B соответственно.

**Заключение.** Предложенный метод снижения потерь в волноводно-микрополосковом переходе осуществляется за счет уменьшения влияния диэлектрической подложки при использовании различных СВЧ-материалов печатных плат. Это позволяет рассматривать разработанный волноводно-микрополосковый переход как перспективный для соединения различных микрополосковых и волноводных устройств миллиметрового диапазона длин волн.

**Ключевые слова:** миллиметровый диапазон длин волн; волноводно-микрополосковый переход; печатная плата; металлический волновод

**Для цитирования:** Широкополосный волноводно-микрополосковый переход зондового типа миллиметрового диапазона длин волн / А. В. Можаровский, О. В. Сойкин, А. А. Артеменко, Р. О. Масленников, И. Б. Вендик // Изв. вузов России. Радиоэлектроника. 2019. Т. 22, № 5. С. 17–32. doi: 10.32603/1993-8985-2019-22-5-17-32

**Конфликт интересов.** Авторы заявляют об отсутствии конфликта интересов.

Статья поступила в редакцию 27.03.2019; принята к публикации после рецензирования 16.08.2019; опубликована онлайн 29.11.2019

**Introduction**. One of the main modern trends in the development of wireless networks is the permanent growth in the volume of transmitted information. This is primarily due to the increasing share of multimedia mobile traffic and the popularity of modern high-resolution video streaming services. To meet present-day high throughput requirements, modern communication systems must support data transfer rates up to units or even tens of gigabits per second. The achievement of such speeds is possible primarily through the use of a wider frequency band of transmitted signals, as well as by developing more efficient ways of using the spectrum. Such methods include, for example, high-order modulations and the implementation of communication systems based on the MIMO (Multiple Input Multiple Output) technology [1], which allows the simultaneous parallel transfer of several data streams using multiple antennas, including also a polarisation diversity.

The main difficulty in allocating a wider frequency band of transmitted signals is an overloaded spectrum in traditional frequency ranges up to 6 GHz. One of the possible approaches to solving this problem is to increase the carrier frequency of the transmitted signals to the millimetre-wavelength range (30…300 GHz). This range allows the use a number of bands with a width of up to several gigahertz for data transmission, which seems sufficient to achieve the required speeds.

For the development of new fixed radio communication systems of millimetre (or close-to millimetre) ranges, the most actively used ranges are 27.5...29.5, 40.5...43.5, 57...64, 71...76/81...86 and 92...95 GHz. Moreover, the frequency range of 57...64 GHz is the most attractive for the implementation of next-generation Wi-Fi systems [2], line-of-sight links for cellular communication systems, fixed wireless access networks, as well as the deployment of 5th generation (5G) mobile networks [3]. The main reason for this is the simplified (or, in a number of countries, completely absent) licensing procedure for frequencies and devices, as well as weakened regulatory restrictions [4–6] due to the oxygen absorption line allocating within this range, which leads to a signifacant (up to 16 dB/km) attenuation of electromagnetic energy during propagation [7]. In view of this, the frequency range of 60 GHz is mostly used for local communication systems designed to work over short distances up to 10–20 m indoors and up to 300–500 m outdoors.

Most of the passive elements of millimetre-wave radiocommunication systems, such as diplexers, circulators, orthomode transducers, as well as external antennas having a high gain, are usually based on hollow metal waveguides or have a waveguide interface. The main advantage of waveguide-based devices is a low insertion loss level comparing to other technologies, as well as high reliability, mechanical stability, the ability to transmit high power signals and the possibility to integrate with communication system housing elements. On the other hand, the vast majority of active elements of the radio frequency path of millimetre-wave communication systems, such as power amplifiers, low-noise amplifiers, mixers, filters, etc., are typically implemented on printed circuit boards and have an interface based on microstrip or other planar transmission lines. Thus, the development of a broadband waveguide-microstrip transition (WMST) for the efficient transmission of signals between the active elements of the radio frequency circuits and the passive elements of the antenna feeding path of communication systems is relevant. In addition, such a transition can be used to test the characteristics of various samples of developed printed circits and devices based on surface mounted elements.

With an increase in the operating frequency to the millimetre-wave range, losses in printed structures increase significantly and therefore the reduction of the losses during the passage of a wave through a transition becomes an important problem. In this case, there is a need to analyse the influence of the properties of the dielectric substrate material and the conductive layers of the printed circuit board on the characteristics of the printed structures, as well as to analyse methods for reducing the negative effect of the properties of the substrate on the characteristics of the developed WMST.

The main requirements for the developed WMST are low insertion losses (less than 1 dB) and the reflection coefficient $S_{11} < -10$ dB in the considered frequency range of 57…64 GHz. Since the WMST is intended for use as part of the radio frequency module of a radio communication system, it must be implemented on a common multilayer printed circuit board together with the active radio frequency circuit elements. For a radio-frequency module implementation several layers of metallisation of a printed circuit board are often used for tracing signal lines, control lines and supplying active components, providing several shielding layers of metallisation necessary for isolation of digital and analogue circuits. The multilayer structure of the printed circuit board provides a compact arrangement of lumped and distributed elements and reduces overall dimensions. For connection to the waveguide components of the antenna path of communication systems in the frequency range 57…64 GHz, as well as to measuring equipment, the transition should have an interface based on a standard rectangular waveguide WR15 with a section size of 3.76 × 1.88 mm.

In order to reduce losses in the transition, the authors studied the effect of the dielectric substrate material and the method of manufacturing copper foil on the characteristics of printed structures implemented on a printed circuit board, including the developed WMST.

A probe-type junction with an additional waveguide back-short based on a shorted section of a regular waveguide WR15 was chosen as the main version of the WMST. The characteristics of the transitions were studied using full-wave simulations in the computer-aided design (CAD) system CST Microwave Studio and confirmed by measuring test samples.

**The effect of the substrate material and the properties of metal foil on the characteristics of printed structures**. The properties of transitions and features of the technology significantly depend on the properties of the materials used. Losses arising in transmission lines on printed circuit boards can be sorted by the nature of the occurrence into losses in conductors and losses in a dielectric substrate.

Losses in conductors occur for several main reasons. The first is the finite electrical conductivity of the metal foil used in the manufacture of printed circuit boards. The current density is maximal at the surface of the conductor, decreasing exponentially within the surface. The depth at which the current density decreases by *e* times, known as the skin depth, is determined by the expression

$$\Delta = \frac{1}{\sqrt{\pi f \mu \sigma}},$$

where $f$ is the frequency; $\sigma$ is the electrical conductivity; $\mu$ is the magnetic permeability of the conductor. With increasing frequency, the thickness of the skin depth decreases, leading to an increase of the current density in the surface layer of the conductor, as well as, consequently, to a significant increase in the active resistance of the conductor and an increase in linear losses. So, with an increase in the signal frequency from 1 to 60 GHz, the thickness of the skin depth of a copper conductor decreases from 2.1 to 0.27 μm. Obviously, with such a small thickness of the skin depth in the millimetre-wave range, surface inhomogeneities caused by the peculiarities of copper foil production become comparable in size to it, significantly affecting losses per unit length in conductors.

Typically, there are 2 types of foil used for the manufacture of printed circuit boards: rolled and electrolytically deposited. Rolled copper foil is obtained from a thick copper billet by successive cold rolling until the desired thickness is achieved [8]. The smoothness of the surface of the foil, usually described by the root-mean-square (RMS) deviation of the grain size, in this case, depends on the characteristics of the rolling machine and usually amounts to tenths of a micrometre, which helps to reduce the heat loss in microwave conductors. On the other hand, a uniform surface reduces the bonding strength of the layers in multilayer printed circuit boards and degrades the adhesion of the printed-circuit resist. In addition, the rolled foil has a horizontal grain structure, which complicates etching in a confined space conductor.

For the manufacture of electrolytically deposited foil, the process of galvanic deposition of copper [8] on a rotating drum made of titanium or stainless steel is used. The thickness of the deposited copper layer is controlled by the rotation speed of the drum. At the same time, the copper surface is smoother and brighter on the drum side, but matte and rougher on the electrolyte deposition side. On the rough side, copper adheres to the dielectric to improve adhesive properties when adhered to the substrate. This approach makes it possible to improve the adhesion of the dielectric and the foil in the core layers, which improves their mechanical properties; however, the rougher side is located in the region with a higher dielectric constant of the surrounding space and, as a result, in the region of higher electric current density due to the "pulling" of the electromagnetic field to dielectric.

Typical roughness values (RMS) for various types of copper foil materials manufactured by Rogers[*1] are 0.3…0.4 μm for rolled foil and 1.8…3.2 μm for the roughened side of the electrolytically deposited foil. For the smooth side of an electrolytically deposited foil, the roughness values are close to those for rolled foil and amount to 0.4…0.5 μm.

In order to study the effect of surface roughness of copper foil on losses per unit length in transmission lines on printed circuit boards, full-wave simulation was performed in the CST Microwave Studio CAD system using an MSL (microstrip line) model with a line impedance of 50 Ohms implemented on a

---

[*1] https://www.rogerscorp.com/documents/749/acs/Copper-Foils-for-High-Frequency-Circuit-Materials.pdf (дата обращения: 29.09.2019).

0.203-mm thick-substrate. A thickness of 18 μm for both metallisation layers (MSL and ground plane) was selected. The loss tangent of the substrate material was set to zero to exclude the influence of losses in the dielectric. The surface roughness of the copper foil was set by introducing a two-layer material with copper conductivity and given parameters RMS* of inhomogeneities both on the dielectric side and on the reverse (smooth) side.

Fig. 1 shows the results of full-wave simulation of losses *l* in the millimetre-wavelength range in an MSL made of smooth (without roughness), rolled and electrolytically deposited copper. As seen from Fig. 1, the introduction of roughness significantly affects the losses in the MSL. According to the simulation results in the considered frequency range, an 0.08 dB/cm losses increase was obtained when using rolled foil and 0.13 dB/cm increase for electrolytically deposited foil compared with losses in the case of using a smooth foil.

Another source of losses in printed circuit boards is a dielectric loss. The most common in the manufacture of microwave printed circuit boards are materials based on a are glass reinforced hydrocarbon laminates with ceramic filler, such as, for example, materials of the RO4000 series*2 and their analogues. The main advantage of such materials is the relatively low cost of their manufacture and the ability to produce multilayer boards and reliable RO4000/FR4 hybrid assemblies.

However, at frequencies of the order of tens of gigahertz, the losses in these materials are quite high. As an alternative, polytetrafluoroethylene (PTFE)-based materials with additional reinforcement with non-woven fiberglass, such as, for example, in RT/Duroid 5880 material*3 or ceramic filler, as in materials of the RO3000 series*4, can be used. The dielectric loss tangent of PTFE-based materials is the lowest among currently available printed circuit board materials, which makes them most suitable for microwave devices where losses should be minimised. The main disadvantage of these materials is their low adhesive properties, which greatly complicates the manyfacturing of multilayer printed circuit boards. For this reason, the fabrication of a multilayer structure usually requires a significant (about 100 °C) increase in temperature, which complicates the process, increases the cost and reduces the yield of suitable samples.

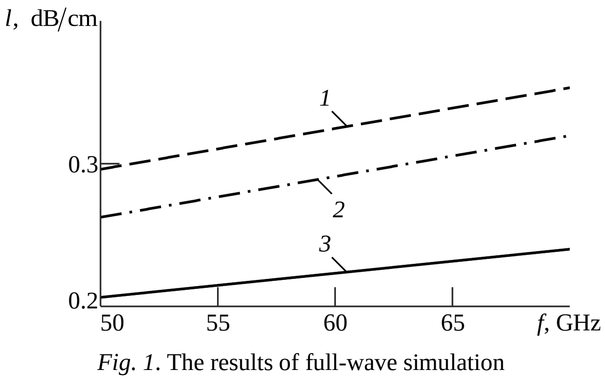


*Fig. 1*. The results of full-wave simulation of a microstrip line with different roughness of the material: *1* – electrolytically deposited copper foil; *2* – rolled copper foil; *3* – smooth foil

It should be noted that most manufacturers of printed circuit board materials indicate in the specifications only the characteristics of materials for frequencies up to 10 GHz; therefore, to analyse the effect of dielectric losses on the characteristics of printed transmission lines, it is important to study the characteristics of the material at higher frequencies. The experimental data on the dielectric permittivity of some popular microwave materials of printed circuit boards manufactured by Rogers are presented, for example, in [9].

In order to study the losses in various dielectric substrates of printed circuit boards, MSL models on substrates made of Rogers materials RO4350B, RO3003, and RT/Duroid 5880 with a line impedance of 50 Ohms were used. During the simulation, the thinnest allowable substrate was chosen for each of the materials from those presented in the specifications (Table 1). This choice is explained, first of all, by the fact that with a decrease in the thickness of the substrate, the width of the MSL with the selected impedance decreases, greatly simplifying the further integration of printed transmission lines with monolithic microwave integrated circuits (MMICs) and surface mount elements, as well as increasing the node packing density.

The results of full-wave analysis of losses for MSL on the substrates indicated in Table 1 are presented in Fig. 2. The solid curves show the results

---

*2 https://www.rogerscorp.com/documents/726/acm/RO4000-Laminates---Data-sheet.pdf (дата обращения: 29.09.2019).

*3 https://www.rogerscorp.com/documents/606/acm/RT-duroid-5870-5880-Data-Sheet.pdf (дата обращения: 29.09.2019).

*4 https://www.rogerscorp.com/documents/722/acs/RO3000-Laminate-Data-Sheet-RO3003-RO3006-RO3010-RO3035.pdf (дата обращения: 29.09.2019).

*Table 1.* Characteristics of microstrip lines, implemented on the materials of the company "Rogers"

| Material | Substrate thickness, mm | Line width, mm | Dielectric permittivity | Dielectric loss tangent at frequency 60 GHz |
|---|---|---|---|---|
| RO4350B | 0.101 | 0.2 | 3.66 | 0.0115 |
| RO3003 | 0.127 | 0.29 | 3.0 | 0.0034 |
| RT/Duroid 5880 | 0.127 | 0.36 | 2.2 | 0.0024 |

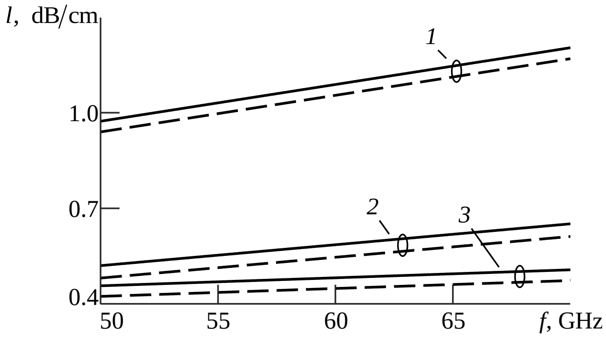


*Fig. 2.* The results of full-wave simulation of a microstrip line on substrates of company "Rogers": *1* – RO4350B; *2* – RO3003; *3* – RT/Duroid 5880. Solid curves – lines based on electrolytically deposited foil; dashed curves – lines based on rolled foil

obtained for an MSL with the characteristics of a foil made by electrolytic deposition; the dashed curves correspond to the results for rolled foil.

In accordance with the simulation results, losses in the dielectric substrate play a decisive role for planar transmission lines made on printed circuit boards in the millimetre-wave range. Nevertheless, for electrically large structures, such as, for example, printed filters, losses in conductors also have a significant effect on the overall level of losses in a planar structure. The obtained results are confirmed by the experimental data presented in a number of works for lower frequencies (see, for example, [10]). Thus, for a material with a small dielectric loss tangent in the low-frequency region, losses in conductors prevail over dielectric losses. However, with increasing frequency, the influence of dielectric losses increases, becoming dominant in the overall level of losses at frequencies above several gigahertz. As a rule, losses in the conductors are proportional to the square root of the frequency, while dielectric losses are proportional to frequency. Although the results presented in [10] were obtained only for the frequency range up to 20 GHz, the observed relations are also valid for higher frequencies.

Thus, based on an analysis of the properties of the dielectric substrate and the metal foil, it can be concluded that in the millimetre-frequency range, the choice of the material of the printed circuit board is a key factor in reducing losses in the structure of printed transmission lines.

**Structure.** There are many options for the implementation of the WMST for millimetre-wave range. For example, the transition can be based on a printed antenna located inside a metal waveguide. The antenna can be a microstrip antenna [11, 12], a printed dipole [13, 14], a quasi-Yagi-Uda antenna [15] or a slot antenna [16, 17]. Typically, transitions of these types provide a wide band of operating frequencies and do not require modifications in the structure of the input waveguide; however, they have a high level of backward radiation, as well as significant losses in the dielectric substrate, which increase with increasing frequency. Another common type of transition comprises those implemented co-directionally with the structure of the input waveguide using a matching metal ridge [18] or based on overlapping strip lines [19], [20]. However, such transitions require modifications in the structure of the waveguide, which must be performed with very high accuracy, leading to a significant increase in manufacturing cost and installation difficulties. In addition, transitions of this type are often can be implemented only on printed circuit boards having a single layer structure, complicating their use in the radio frequency modules, which are usually implemented on multilayer printed circuit boards. A possible solution to this problem consists in the use of printed circuit boards based on combinations of zones having both a single-layer and a multi-layer structure [21]. However, this significantly complicates the manufacturing process of printed circuit boards, as well as increasing the manufacturing cost.

One of the most common types of millimetre-wavelength range WMST is probe-type transitions, in which a conductive probe is located in the structure of the waveguide channel, implemented on a printed circuit board and connected to the MSL [22–24]. A printed circuit board having a probe structure is typically located between the input waveguide, which can comprise the interface of a waveguide diplexer, an orthomode transducer or antenna and additional waveguide back-short (quarter-wavelength shorted segment of the waveguide). The back-short provides in-phase addition of the incident wave from the input waveguide and the wave reflected from the

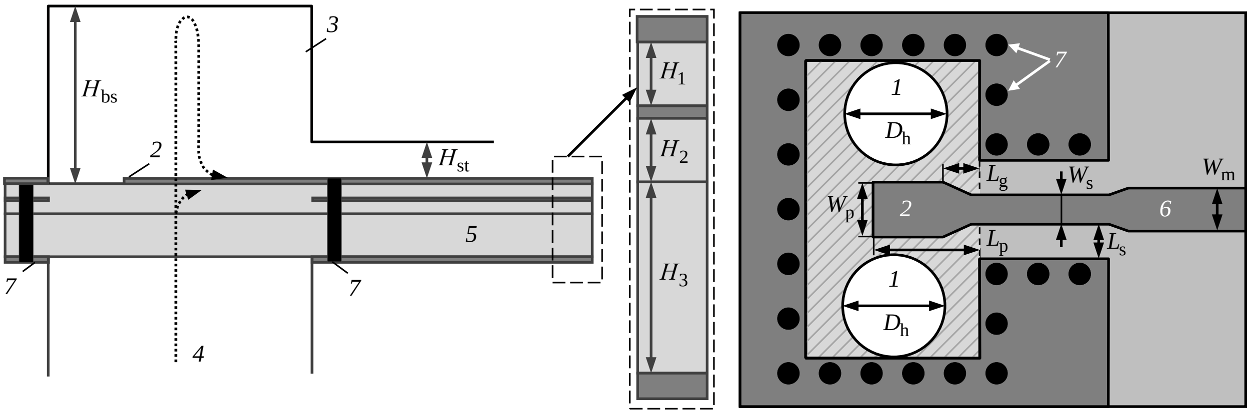


*Fig. 3*. The structure of the probe type transition: *a* – section; *b* – top view
(*1* – perforating non-metallic holes; *2* – probe; *3* – quarter-wave cap; *4* – supply waveguide WR-15; *5* – printed circuit board; *6* – microstrip line; *7* – vias)

waveguide back-short on the conductive probe (Fig. 3, *a*). Typically, probe-type WMSTs have low insertion loss and a wide operational frequency band, as well as providing a low level of spurious radiation, which makes them very attractive for use in millimetre-wave communication systems. The main disadvantage of the presented WMST design is the presence of a thick multilayer dielectric substrate through which the wave passes in the region of the waveguide channel. With an increase in the operating frequency, the dielectric progressively affects the transition characteristics, significantly increasing losses. In addition, the printed circuit board dielectric introduces additional parasitic capacitive reactance between the input waveguide and the conductive probe, complicating the impedance matching and narrowing the operational bandwidth [25]. In order to compensate the parasitic effect of the printed circuit board material, as well as improving the matching in the probe-type WMST, various matching circuits are typically used, which can be based, for example, on MSL sections [26], complex matching chains [27] or cutouts in a number of dielectric layers [28]. The main disadvantage of the described approaches is their inherently complex structure due to which a noticeable narrowing of the operational frequency band occurs.

In this work, in order to reduce the influence of a thick dielectric substrate on the transition characteristics, non-metallised through holes were used in the region of the waveguide channel [29]. The use of holes allows the proportion of dielectric material in the transition region to be reduced, thereby reducing all the earlier-described negative effects of the influence of the dielectric substrate. The holes, having a diameter of $D_h$, are of round shape and symmetrically located around the conductive probe (Fig. 3, *b*). The choice of the shape of the holes is justified by the simplicity of their manufacturing by drilling, which is suitable for mass production since the cost of production of printed circuit boards is not increased. When designing the transition, holes of a different shape were also studied; however, when using them, a significant improvement in the characteristics of the transition was not achieved in comparison with round holes. The diameter and position of the holes were optimised using full-wave simulation to reduce insertion loss and improve the reflection coefficient.

The three-dimensional model of the probe-type transition is shown in Fig. 4. The transition is based on a combination of a printed circuit board containing a conductive probe located between a standard WR15 input waveguide with a cross-section of 3.76 × 1.88 mm and a waveguide back-short of the same cross-section with a length of a quarter wavelength in the considered frequency range. In the area of the waveguide channel, metallisation is removed from all layers of the printed circuit board (except for

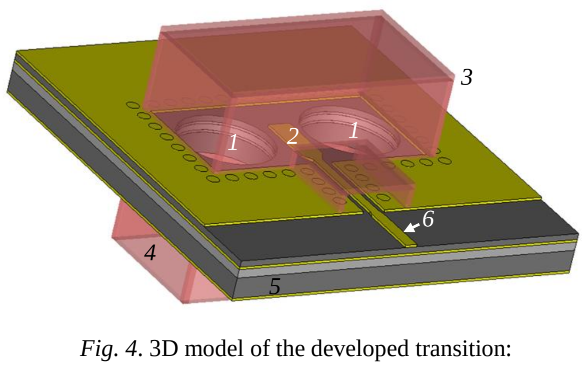


*Fig. 4*. 3D model of the developed transition:
*1* – perforating non-metallic holes; *2* – probe; *3* – quarter-wave cap; *4* – supply waveguide; *5* – printed circuit board; *6* – microstrip line

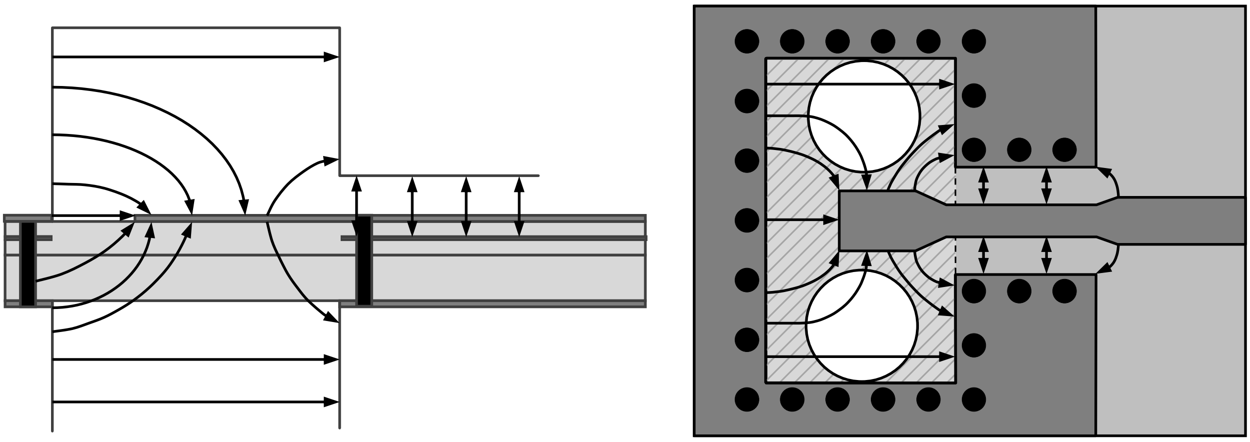

*Fig. 5.* The structure of the electric field of the probe waveguide microstrip transition

the probe) for the free passage of electromagnetic waves from the input waveguide. Metallised via holes are located along the contour of the input waveguide and effectively extend the waveguide channel in the body of the board to electrically connect the input waveguide and the quarter-wave back-short. At the same time, they provide reliable shielding of the transition structure and prevent signal leakage or spurious radiation. The diameter of the metallised via holes is 0.2 mm, with a distance between the centres of about 0.4 mm. To prevent reflection in the region where the section of the waveguide back-short is located above the MSL, forming a quasi-strip asymmetric line structure, narrowing was implemented to compensate for this effect. The structure of electric fields in a probe-type WMST is presented in Fig. 5.

To assess the effect of the properties of the dielectric substrate on the characteristics of the waveguide-microstrip junction, its structure was implemented on two different printed circuit board based on Rogers 4350B material (low cost, ease of manufacture and applicability for mass production; however, the dielectric loss tangent is quite large in the millimetre-wave range) and Rogers RT/Duroid 5880 material (the smallest dielectric loss tangent in the millimetre-wave range; however, involving a high cost and complexity of multilayer printed circuit board manufacturing).

The structure of both boards, which corresponds to that shown in Fig. 3, *a*, is made on three layers of a dielectric and four layers of metallisation. For both printed circuit boards, dielectric cores located on the outer layers of the printed circuit board are separated by one prepreg layer (Rogers 4450B for a board based on RO4350B and TacBond 1.5 for a board based on RT/Duroid 5880). The dimensions of the individual elements and the thickness of the dielectric layers for both printed circuit boards are presented in Table 2.

*Table 2.* Dimensions of waveguide microstrip junctions implemented on printed circuit boards from Rogers materials

| Dimensions, mm (see Fig. 3) | RO4350B | RT/Duroid 5880 |
|---|---|---|
| $W_p$ | 0.38 | 0.35 |
| $L_p$ | 1.22 | 1.0 |
| $W_s$ | 0.15 | 0.2 |
| $L_s$ | 0.115 | 0.15 |
| $W_m$ | 0.2 | 0.36 |
| $L_g$ | 0.27 | 0.2 |
| $D_h$ | 1.55 | 1.4 |
| $H_{bs}$ | 1.27 | 1.2 |
| $H_{st}$ | 0.3 | 0.3 |
| $H_1$ | 0.101 | 0.127 |
| $H_2$ | 0.1 | 0.144 |
| $H_3$ | 0.338 | 0.381 |

**Results of full-wave simulation of probe-type transition.** The probe-type WMST on substrates based on the Rogers RO4350B and RT/Duroid 5880 materials were studied using full-wave simulations in the CAD software CST Microwave Studio. During simulations, the characteristics of the substrate were set in accordance with Table 1. For transition models in all cases, the properties of the conductive layers of the printed circuit board were set in accordance with the characteristics of copper foil made by electrolytic deposition. Aluminium was used as the material for the section of the WR-15 input waveguide and the back-short.

A comparison of the results of simulated *S*-parameters for both transitions is presented in Fig. 6. As follows from the simulation results, transitions in the considered frequency range 57…64 GHz are consistent in terms of the reflection coefficient

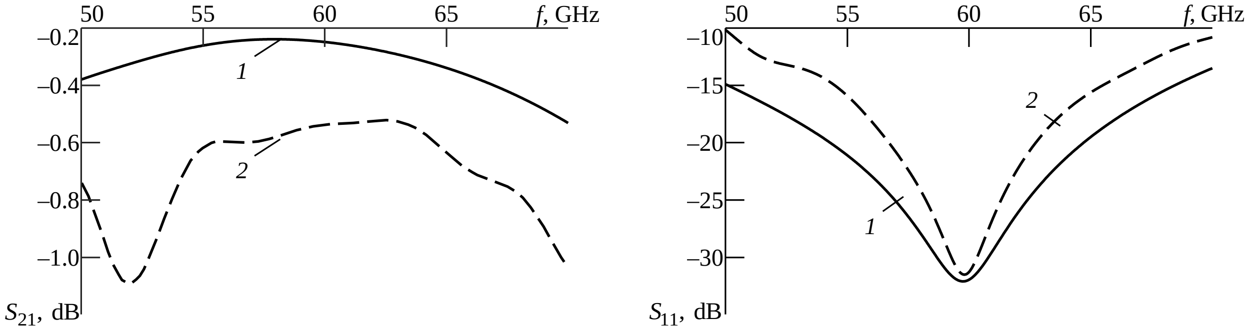


*Fig. 6.* Results of electrodynamic modeling of coefficients of transmission $S_{21}$ and reflection $S_{11}$ of probe waveguide-microstrip transitions. Backing materials: *1* – RT/Duroid 5880; *2* – RO4350B

$S_{11} < -17$ dB and $S_{11} < -21$ dB for transitions based on the materials RO4350B and RT/Duroid 5880, respectively. In addition, both transitions are provide the reflection coefficient $S_{11} < -10$ dB over the entire frequency band 50…70 GHz. The level of the transmission coefficient in the frequency range 57…64 GHz was $S_{21} > -0.6$ and –0.35 dB, respectively.

**Experimental studies of prototypes of probe-type transitions.** The experimental verification of the designed transitions was performed on the prototypes of the back-to-back transitions "waveguide–MSL–waveguide". For each of the transitions, back-to-back implementations with different MSL lengths were fabricated. This approach made it possible to experimentally estimate the insertion loss per unit length in the MSL that can be further used to determine the characteristics of individual transitions. The MSL lengths for fabricated back-to-back transitions are 25 and 35 mm for transitions based on the material RO4350B and 25 and 40 mm for transitions based on RT/Duroid 5880 (Fig. 7). Rolled foil is used in experimental mock transitions to reduce the level of losses.

Experimental studies are performed using the Rhode & Schwarz ZVA24 vector network analyser with ZVA-Z90E external upconverting mixers. The specified equipment allows measurements in the frequency range 57…95 GHz, which is enough to study the developed transitions.

A comparison of the reflection and transmission coefficients measured and obtained from the results $S_{11}$ of full-wave simulations $S_{21}$ for back-to-back WMSTs is presented in Fig. 8 for transitions based on RO4350B and in Fig. 9 for transitions on RT/Duroid 5880.

For back-to-back transitions, a good agreement was achieved between the simulation results and measurement both for the reflection coefficient $S_{11}$ and for the transmission coefficient $S_{21}$. Thus, according to the measurement results, with the exception of a number of points, for all back-to-back transitions the level of the reflection coefficient $S_{11} < -10$ dB is achieved in the frequency band

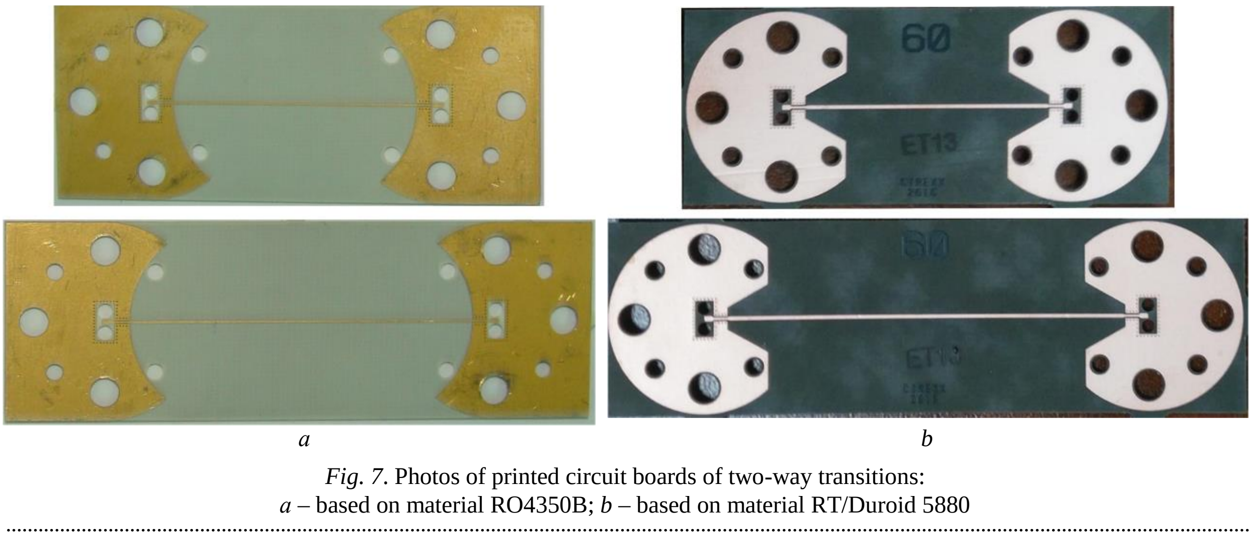


*a* *b*

*Fig. 7.* Photos of printed circuit boards of two-way transitions:
*a* – based on material RO4350B; *b* – based on material RT/Duroid 5880

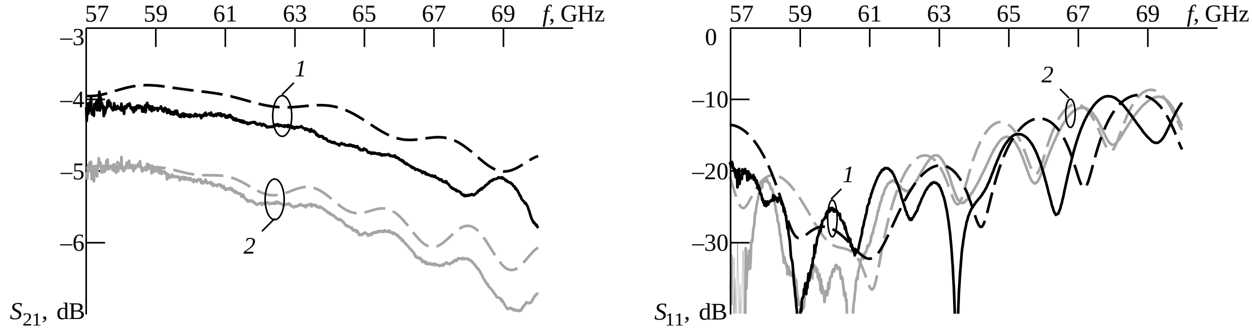


*Fig. 8*. Comparison of the results of modeling and measuring coefficients of the transmission $S_{21}$ and reflection $S_{11}$ of double-sided waveguide-microstrip junctions based on RO4350B.
Microstrip length: *1* – 25 mm; *2* – 35 mm.
Solid lines – simulation results; dashed lines – measurement results

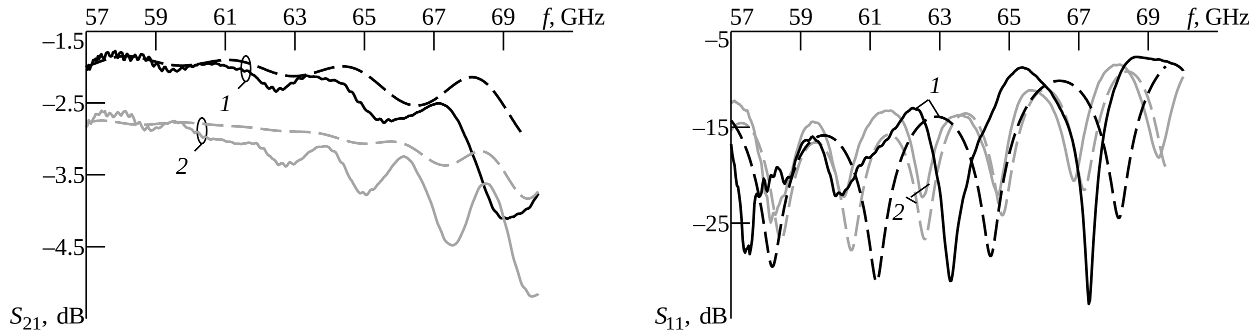


*Fig. 9*. Comparison of the results of modeling and measuring coefficients of the transmission $S_{21}$ and reflection $S_{11}$ of double-sided waveguide-microstrip junctions based on RT/Duroid 5880.
Microstrip length: *1* – 25 mm; *2* – 40 mm.
Solid lines – simulation results; dashed lines – measurement results

57…70 GHz. An increase in the reflection coefficient compared to a single transition (Fig. 6) is caused by reflections between the transitions in “waveguide–MSL–waveguide” structure. However, a good agreement between the measured *S*-parameters of the test structures and the simulation results leads to the conclusion that, for an individual transition, the reflection coefficient values should also be close to those shown in Fig. 6.

The loss per unit length in the MSL with an impedance of 50 Ohms are estimated according to the results of measurements of back-to-back transitions with different lengths of the MSL. In the frequency band 57…64 GHz, they amounted to 1.1 dB for a line on a substrate of RO4350B material and 0.55 dB for a line on a substrate of RT/Duroid 5880 material, which is in good agreement with the results of full-wave simulations for MSL made of copper foil made by electrolytic deposition. Taking the measured losses in the MSL into account, it is possible to determine the insertion loss for an individual transition. Thus, according to the results of measurements in the frequency range 57…64 GHz, insertion loss in the developed transitions are 0.4 dB and 0.7 dB for materials RT/Duroid 5880 and RO4350B, respectively, which is also in good agreement with the simulation results. Googrepetability of the results were obtained from the measurements carried out for several samples of the manufactured transitions, demonstrating the stability of the characteristics of the developed WMST in terms of manufacturing inaccuracies and its applicability to mass production.

**Conclusion.** The problem of developing a wideband probe-type WMST for the frequency range of 60 GHz has been considered. A distinctive feature of the transition is the use of non-metallised through holes in the printed circuit board, symmetrically located around the probe. These holes can reduce the fraction of the lossy dielectric material in the waveguide channel and, thereby, reduce losses in the transition to ensure good matching of the input waveguide and the MSL. The transition structure has been adapted to the use of printed circuit boards. Analysis of losses in metal foil and dielectric material justified the choice of dielectric and the foil manufacturing method. As a result, the transition was made using two common microwave materials manufactured by Rogers: RO4350B and RT/Duroid 5880.

In order to conduct the experimental studies, mock-ups of "waveguide–MSL–waveguide" back-to-back transitions were made on printed circuit boards using selected materials. Measurements of the back-to-back transition confirmed the results of preliminary full-wave simulations. The operational frequency band of the developed transitions in terms of the reflection coefficient $S_{11} < -10$ dB amounted to more than 20%. For the RT/Duroid 5880 material, the loss per unit length in the MSL was 0.55 dB/cm, while the insertion loss in transition was 0.4 dB; for the RO4350B these losses are 1.1 and 0.7 dB, respectively. As a result of the study, the problem of providing a low loss in the WMST operating in the frequency range of 57…64 GHz was solved due to the use of high-frequency materials of printed circuit boards with rolled foil and additional non-metallised through holes in the transition structure. The results show that the proposed transition design allows low insertion loss values to be achieved by reducing the influence of the dielectric substrate when using various high-frquiency printed circuit board materials.

## Authors' contribution

**Andrey V. Mozharovskiy,** the study of methods to reduce the influence of the dielectric substrate on the characteristics of the designed transition. Experimental study of the fabricated transition samples. Preparation of the paper text.

**Oleg V. Soykin,** the study of methods to reduce the influence of the dielectric substrate on the characteristics of the developed transition. An experimental study of the fabricated transition samples.

**Aleksey A. Artemenko,** full-wave simulation of the developed transition.

**Roman O. Maslennikov,** management of the work.

**Irina B. Vendik,** management of the work. Preparation of the paper text.

## Авторский вклад

**Можаровский А. В. –** исследование влияния материала подложки и свойств металлической фольги на характеристики переходов между металлическим волноводом и микрополосковой линией передачи. Расчет характеристик разработанного перехода с помощью электродинамического моделирования. Экспериментальное исследование изготовленных макетов переходов. Подготовка текста статьи.

**Сойкин О. В. –** исследование методов уменьшения влияния диэлектрической подложки на характеристики разработанного перехода. Экспериментальное исследование изготовленных макетов переходов.

**Артеменко А. А. –** электродинамическое моделирование разработанного перехода.

**Масленников Р. О. –** руководство работой.

**Вендик И. Б. –** руководство работой. Подготовка текста статьи.

## References

1. Boccardi F., Heath R. W., Lozano A., Marzetta T. L., Popovski P. Five Disruptive Technology Directions for 5G. IEEE Communications Magazine. 2014, vol. 52, iss. 2, pp. 74–80. doi: 10.1109/MCOM.2014.6736746

2. 802.11-2016. IEEE Standard for Information technology – Telecommunications and information exchange between systems Local and metropolitan area networks – Specific requirements – Pt 11: Wireless LAN Medium Access Control (MAC) and Physical Layer (PHY) Specifications. doi: 10.1109/IEEESTD.2016.7786995

3. Rappaport T. S., Sun S., Mayzus R., Zhao H., Azar Y., Wang K., Wong G. N., Schulz J. K., Samimi M., Gutierrez F. Millimeter Wave Mobile Communications for 5G Cellular: It Will Work! IEEE Access (Invited). 2013, vol. 1, pp. 335–349. doi: 10.1109/ACCESS.2013.2260813

4. Decision of the State Committee for Emergencies of 12.12.2011 no. 11-13-06-1. On the Use by Radio-Electronic Means of the Fixed Service of the Radio Frequency Band 57–64 GHz. Available at: http://grfc.ru/upload/medialibrary/713/Reshenie_GKRCH_ot_10.03.2017_17_40_03_15.02.2019.docx (accessed: 29.09.2019)

5. ETSI EN 302 217-3 V2.2.1 (2014-04): Harmonized European Standard. Available at: https://www.etsi.org/deliver/etsi_en/302200_302299/30221703/02.02.01_60/en_30221703v020201p.pdf (accessed: 29.09.2019)

6. Revision of Part 15 of the Commission's Rules Regarding Operation in the 57–64 GHz Band. Available at: http://fjallfoss.fcc.gov/edocs_public/attachmatch/FCC-13-112A1.pdf (accessed: 29.09.2019)

7. Stevens M., Grafton G. The Benefits of 60 GHz Unlisensed Wireless Communications. 10 p. Available at: https://www.faltmann.de/pdf/white-paper-benefits-of-60ghz.pdf (accessed: 15.02.2019)

8. Bogdanov Yu., Kochemasov V., Khas'yanova E. Foil Dielectrics – How to Choose the Best Option for RF / Microwave Circuit Boards. *Pechatnyi montazh* [Printed Wiring]. 2013, no. 3, pp. 142–147. (In Russ.)

9. Felbecker R., Keusgen W., Peter M. Estimation of Permittivity and Loss Tangent of High Frequency Materials in the Millimeter Wave Band Using a Hemispherical Open Resonator. IEEE Intern. Conf. on Microwaves, Communications, Antennas and Electronics Systems (COMCAS 2011). Tel Aviv, Israel, 7–9 Nov. 2011, pp. 1–8. doi: 10.1109/COMCAS.2011.6105829

10. Liew E., Okubo T.-A., Sudo T., Hosoi T., Tsuyoshi H., Kuwako F. Signal Transmission Loss Due to Copper Surface Roughness in High-Frequency Region. IPC APEX EXPO 2014. Las Vegas, 25–27 March 2014. Available at: http://www.circuitinsight.com/pdf/signal_transmission_loss_copper_surface_roughness_ipc.pdf (accessed: 29.09.2019)

11. Artemenko A., Maltsev A., Maslennikov R., Sevastyanov A., Ssorin V. Design of Wideband Waveguide to Microstrip Transition for 60 GHz Frequency Band. Proc. of 41st European Microwave Conference (EuMC), Manchester (UK), 10–13 Oct. 2011, pp. 838–841.

12. Ishikawa Y., Sakakibara K., Suzuki Y., Kikuma N. Millimeter-Wave Topside Waveguide-to-Microstrip Transition in Multilayer Substrate. IEEE Microwave and Wireless Components Letters. 2018, vol. 28, iss. 5, pp. 380–382. doi: 10.1109/LMWC.2018.2812125

13. Kook J. L., Dong H. L., Rieh J.-S., Kim M. A V-band Waveguide Transition Design Appropriate for Monolithic Integration. Proc. of Asia-Pacific Microwave Conf. (APMC). Bangkok, Thailand, 11–14 Dec. 2007, pp. 1–4. doi: 10.1109/APMC.2007.4554756

14. Kim J., Choe W., Jeong J. Submillimeter-Wave Waveguide-to-Microstrip Transitions for Wide Circuits/Wafers. IEEE Trans. on Terahertz Science and Technology. 2017, vol. 7, iss. 4, pp. 440–445. doi: 10.1109/TTHZ.2017.2701151

15. Kaneda N., Qian Y., Itoh T. A Broad-Band Microstrip-to-Waveguide Transition Using Quasi-Yagi Antenna. IEEE Trans. on Microwave Theory and Techniques. 1999, vol. 47, iss. 12, pp. 2562–2567. doi: 10.1109/22.809007

16. Aliakbarian H., Enayati A., Yousefbeigi M., Shahabadi M. Low-Radiation-Loss Waveguide-to-Microstrip Transition Using a Double Slit Configuration for Mi-crostrip Array Feeding. Asia-Pacific Microwave Conf. Bangkok, Thailand, 11–14 Dec. 2007. Piscataway, IEEE, 2007, pp. 737–740. doi: 10.1109/APMC.2007.4554952

17. Aliakbarian H., Enayati A., Yousefbeigi M., Shahabadi M. Low-Radiation-Loss Waveguide-to-Microstrip Transition Using a Double Slit Configuration for Microstrip Array Feeding. Asia-Pacific Microwave Conf. Bangkok, Thailand, 11–14 Dec. 2007. doi: 10.1109/APMC.2007.4554952

18. Zhou Y., Liu H., Li E., Guo G., Yang T. Design of a Wideband Transition from Double-Ridge Waveguide to Microstrip Line. Intern. Conf. on Microwave and Millimeter Wave Technology. Chengdu, China, 8–11 May 2010. Piscataway, IEEE, 2010. doi: 10.1109/icmmt.2010.5525049

19. Mozharovskiy A., Artemenko A., Ssorin V., Maslennikov R., Sevastyanov A. Wideband Tapered Antipodal Fin-Line Waveguide-to-Microstrip Transition for E-band Applications. Proc. of 43st Europ. Microwave Conf. (EuMC). Nuremberg, Germany, 6–10 Oct. 2013. In 3 Vols, vol. 3, pp. 1187–1190.

20. Zhang C. W. A Novel W-Band Waveguide-To-Microstrip Antipodal Finline Transition. IEEE Intern. Conf. on Applied Superconductivity and Electromagnetic Devices. Beijing, China, 25–27 Oct. 2013, pp. 166–168. doi: 10.1109/ASEMD.2013.6780735

21. Mozharovskiy A., Artemenko A., Sevastyanov A., Ssorin V., Maslennikov R. Beam-Steerable Integrated Lens Antenna with Waveguide Feeding System for 71-76/81-86 GHz point-to-point Applications. 10th Europ. Conf. on Antennas and Propagation (EuCAP). Davos, Switzerland, 10–15 April 2016. doi: 10.1109/EuCAP.2016.7481774

22. Sakakibara K., Hirono M., Kikuma N., Hirayama H. Broadband and Planar Microstrip-to-Waveguide Transitions in Millimeter-Wave Band. Intern. Conf. on Microwave and Millimeter Wave Technology. Nanjing, China, 21–24 April 2008, Piscataway, IEEE, 2008. doi: 10.1109/ICMMT.2008.4540667

23. Sakakibara K., Hirono M., Kikuma N., Hirayama H. Broadband and Planar Microstrip-To-Waveguide Transitions in Millimeter-Wave Band. Intern. Conf. on Microwave and Millimeter Wave Technology. Nanjing, China, 21–24 April 2008. doi: 10.1109/ICMMT.2008.4540667

24. Tikhov Y., Moon J.-W., Kim Y.-J., Sinelnikov Y. Refined Characterization of E-Plane Waveguide to Microstrip Transition for Millimeter-Wave Applications. Asia-Pacific Microwave Conf. Sydney, NSW, Australia, 3–6 Dec. 2000, pp. 1187–1190. doi: 10.1109/APMC.2000.926043

25. Soykin O., Artemenko A., Ssorin V., Mozharovskiy A., Maslennikov R. Wideband Probe-Type Waveguide-to-Microstrip Transition for V-band Applications. Proc. of 46th Europ. Microwave Conf. (EuMC). London, UK, 4–6 Oct. 2016, pp. 1–4. doi: 10.1109/EuMC.2016.7824262

26. Shireen R., Shi S., Prather D. W. W-Band Microstrip-to-Waveguide Transition Using Via Fences. Progress In Electromagnetics Research Letters. 2010, vol. 16, pp. 151–160.

27. Tahara Y., Ohno A., Oh-hashi H. , Makino S., Ono M., Ohba T. A Novel Microstrip-to-Waveguide Transition Using Electromagnetic Bandgap Structures. Proc. of Intern. Symp. on Antennas and Propagation (ISAP), 2005, pp. 459–462.

28. Pat. US 6 967 542 B2. Int. Cl. H01P 5/107; H01P 5/10; H01P 005/107 (2006.01). Weinstein M. E. Microstrip-Waveguide Transition. Publ. 2005/11/22.

29. Soikin O. V., Ssorin V. N., Mozharovskii A. V., Artemenko A. A., Maslennikov R. O. Waveguide Microstrip Junction. Pat. RF 2 600 506 C1. H01P 5/107 (2006.01). Publ. 20.10.2016. Bul. 29. (In Russ.)

## Information about the authors

**Andrey V. Mozharovskiy,** Senior microwave systems and antennas engineer in LLC "Radio Gigabit". He graduated from Lobachevsky State University of Nizhny Novgorod (2011) with a degree in "Information Systems and Technologies". He is a PhD student of the Department of Microradioelectronics and Radio Technology at Saint Petersburg Electrotechnical University. The author of 30 scientific publications. Area of expertise: various millimeter wavelength range antenna and feeding systems, including printed, waveguide and lens antennas and antenna arrays; planar and waveguide duplexing devices and filters.
Address: LLC "Radio Gigabit", 95 bld. 2, Osharskaya Str., Nizhny Novgorod 603105, Russia
E-mail: andrey.mozharovskiy@radiogigabit.com
https://orcid.org/0000-0002-9827-6720

**Oleg V. Soykin,** Master Sci. (2014) on Radiophysics, Researcher in LLC "Radio Gigabit". The author of 13 scientific publications. Area of expertise: antenna systems for wireless communication systems; microwave transmission lines/antennas and other passive devices; millimeter wavelength devices.
Address: LLC "Radio Gigabit", 95 bld. 2, Osharskaya Str., Nizhny Novgorod 603105, Russia
E-mail: oleg.soykin@radiogigabit.com

**Aleksey A. Artemenko,** Cand. Sci. (Eng.) (2013), R&D director in LLC "Radio Gigabit". The author of more than 50 scientific publications. Area of expertise: antenna technology, including aperture antennas, especially millimeter-wave antennas, antenna arrays, printed antennas, and electronically controlled antennas; microwave technology, including passive devices and active radio frequency modules, such as waveguide-to-microstrip transitions, polarization selectors, filters on metal and surface mounted waveguides; microwave transceivers on a modern electronic component base in frequency bands from 0 to 90 GHz.
Address: LLC "Radio Gigabit", 95 bld. 2, Osharskaya Str., Nizhny Novgorod 603105, Russia
E-mail: alexey.artemenko@radiogigabit.com

**Roman O. Maslennikov,** Cand. Sci. (Phys.-Math.) (2012), CEO in LLC "Radio Gigabit". The author of more than 100 scientific publications. Area of expertise: optimal signal processing algorithms in modern wireless communication systems.
Address: LLC "Radio Gigabit", 95 bld. 2, Osharskaya Str., Nizhny Novgorod 603105, Russia
E-mail: roman.maslennikov@radiogigabit.com

**Irina B. Vendik,** Dr. Sci. (Eng.) (1991), Professor (1993) of the Department of Microradioelectronics and Radio Technology of Saint Petersburg Electrotechnical University, Head of the Laboratory of Microwave Microelectronics named university. She is a member of a number of international communities, including IEEE (senior member) and EuMA. The author of more than 300 scientific publications. Area of expertise: properties of materials for electronics (superconductors, ferroelectrics, metamaterials); microwave and terahertz devices.
Address: Saint Petersburg Electrotechnical University, 5 Professor Popov Str., St Petersburg 197376, Russia
E-mail: ibvendik@rambler.ru
https://orcid.org/0000-0001-5632-1223

## Список литературы

1. Five Disruptive Technology Directions for 5G / F. Boccardi, R. W. Heath, A. Lozano, T. L. Marzetta, P. Popovski // IEEE Communications Magazine. 2014. Vol. 52, iss. 2. P. 74–80. doi: 10.1109/MCOM.2014.6736746

2. 802.11-2016. IEEE Standard for Information technology – Telecommunications and information exchange between systems Local and metropolitan area networks – Specific requirements. Pt. 11: Wireless LAN Medium Access Control (MAC) and Physical Layer (PHY) Specifications. doi: 10.1109/IEEESTD.2016.7786995

3. Millimeter Wave Mobile Communications for 5G Cellular: It Will Work! / T. S. Rappaport, S. Sun, R. Mayzus, H. Zhao, Y. Azar, K. Wang, G. N. Wong, J. K. Schulz, M. Samimi, F. Gutierrez // IEEE Access (Invited). 2013. Vol. 1. P. 335–349. doi: 10.1109/ACCESS.2013.2260813

4. Решение ГКРЧ от 20.12.2011 № 11-13-06-1. Об использовании радиоэлектронными средствами фиксированной службы полосы радиочастот 57–64 ГГц (в ред. от 10.03.2017 г. № 17-40-03). URL: http://grfc.ru/upload/medialibrary/713/Reshenie_GKRCH_ot_10.03.2017_17_40_03_15.02.2019.docx (дата обращения: 29.09.2019)

5. ETSI EN 302 217-3 V2.2.1 (2014-04): Harmonized European Standard. URL: https://www.etsi.org/deliver /etsi_en/302200_302299/30221703/02.02.01_60/en_30221703v020201p.pdf (дата обращения: 29.09.2019)

6. Revision of Part 15 of the Commission's Rules Regarding Operation in the 57–64 GHz Band. URL: http://fjallfoss.fcc.gov/edocs_public/attachmatch/FCC-13-112A1.pdf (дата обращения: 29.09.2019)

7. Stevens M., Grafton G. The Benefits of 60 GHz Unlisensed Wireless Communications. 10 p. URL: https://www.faltmann.de/pdf/white-paper-benefits-of-60ghz.pdf (дата обращения: 15.02.2019)

8. Богданов Ю., Кочемасов В., Хасьянова Е. Фольгированные диэлектрики – как выбрать оптимальный вариант для печатных плат ВЧ/СВЧ–диапазонов // Печатный монтаж. 2013. № 3. С. 142–147.

9. Felbecker R., Keusgen W., Peter M. Estimation of permittivity and loss tangent of high frequency materials in the millimeter wave band using a hemispherical open resonator // IEEE Intern. Conf. on Microwaves, Communications, Antennas and Electronics Systems (COMCAS 2011), Tel Aviv, Israel, 7–9 Nov. 2011. P. 1–8. doi: 10.1109/COMCAS.2011.6105829

10. Signal transmission loss due to copper surface roughness in high-frequency region / E. Liew, T.-A. Okubo, T. Sudo, T. Hosoi, H. Tsuyoshi, F. Kuwako // IPC APEX EXPO 2014, Las Vegas, 25–27 March 2014. URL: http://www.circuitinsight.com/pdf/signal_transmission_loss_copper_surface_roughness_ipc.pdf (дата обращения: 29.09.2019)

11. Design of wideband waveguide to microstrip transition for 60 GHz frequency band / A. Artemenko, A. Maltsev, R. Maslennikov, A. Sevastyanov, V. Ssorin // Proc. of 41st European Microwave Conference (EuMC), 2011, Manchester, UK, 10–13 Oct. 2011. P. 838–841.

12. Millimeter-Wave Topside Waveguide-to-Microstrip Transition in Multilayer Substrate / Y. Ishikawa, K. Sakakibara, Y. Suzuki, N. Kikuma // IEEE Microwave and Wireless Components Letters. 2018. Vol. 28, iss. 5. P. 380–382. doi: 10.1109/LMWC.2018.2812125

13. A V-band Waveguide Transition Design Appropriate for Monolithic Integration / J. L. Kook, H. L. Dong, J.-S. Rieh, M. Kim // Proc. of Asia-Pacific Microwave Conf. (APMC), Bangkok, Thailand, 11–14 Dec. 2007. P. 1–4. doi: 10.1109/APMC.2007.4554756

14. Kim J., Choe W., Jeong J. Submillimeter-Wave Waveguide-to-Microstrip Transitions for Wide Circuits/Wafers // IEEE Trans. on Terahertz Science and Technology. 2017. Vol. 7, iss. 4. P. 440–445. doi: 10.1109/TTHZ.2017.2701151

15. Kaneda N., Qian Y., Itoh T. A broad-band Microstrip-to-Waveguide Transition Using Quasi-Yagi Antenna // IEEE Trans. on Microwave Theory and Techniques. 1999. Vol. 47, iss. 12. P. 2562–2567. doi: 10.1109/22.809007

16. Low-Radiation-Loss Waveguide-to-Microstrip Transition Using a Double Slit Configuration for Microstrip Array Feeding / H. Aliakbarian, A. Enayati, M. Yousefbeigi, M. Shahabadi // Asia-Pacific Microwave Conf. Bangkok, Thailand, 11–14 Dec. 2007. Piscataway: IEEE, 2007. P. 737–740. doi: 10.1109/APMC.2007.4554952

17. Low-Radiation-Loss Waveguide-to-Microstrip Transition Using a Double Slit Configuration for Microstrip Array Feeding / H. Aliakbarian, A. Enayati, M. Yousefbeigi, M. Shahabadi // Asia-Pacific Microwave Conf., Bangkok, Thailand, 11–14 Dec. 2007. doi: 10.1109/APMC.2007.4554952

18. Design of a Wideband Transition from Double-Ridge Waveguide to Microstrip Line / Y. Zhou, H. Liu, E. Li, G. Guo, T. Yang // Intern. Conf. on Microwave and Millimeter Wave Technology, Chengdu, China, 8–11 May 2010. Piscataway: IEEE, 2010. doi: 10.1109/icmmt.2010.5525049

19. Wideband Tapered Antipodal Fin-Line Waveguide-to-Microstrip Transition for E-band Applications / A. Mozharovskiy, A. Artemenko, V. Ssorin, R. Maslennikov, A. Sevastyanov // Proc. of 43st Europ. Microwave Conf. (EuMC), Nuremberg, Germany, 6–10 Oct. 2013. In 3 Vols. Vol. 3. P. 1187–1190.

20. Zhang C. W. A Novel W-Band Waveguide-To-Microstrip Antipodal Finline Transition // IEEE Intern. Conf. on Applied Superconductivity and Electromagnetic Devices. Beijing, China, 25–27 Oct. 2013. P. 166–168. doi: 10.1109/ASEMD.2013.6780735

21. Beam-Steerable Integrated Lens Antenna with Waveguide Feeding System for 71-76/81-86 GHz point-to-point Applications / A. Mozharovskiy, A. Artemenko, A. Sevastyanov, V. Ssorin, R. Maslennikov // 10th Europ. Conf. on Antennas and Propagation (EuCAP), Davos, Switzerland, 10–15 Apr. 2016. doi: 10.1109/EuCAP.2016.7481774

22. Broadband and Planar Microstrip-to-Waveguide Transitions in Millimeter-Wave Band / K. Sakakibara, M. Hirono, N. Kikuma, H. Hirayama // Intern. Conf. on Microwave and Millimeter Wave Technology, Nanjing, China, 21–24 Apr. 2008. Piscataway: IEEE, 2008. doi: 10.1109/ICMMT.2008.4540667

23. Broadband and planar microstrip-to-waveguide transitions in millimeter-wave band / K. Sakakibara, M. Hirono, N. Kikuma, H. Hirayama // Intern. Conf. on Microwave and Millimeter Wave Technology, Nanjing, China, 21–24 Apr. 2008. doi: 10.1109/ICMMT.2008.4540667

24. Refined characterization of E-plane waveguide to microstrip transition for millimeter-wave applications / Y. Tikhov, J.-W. Moon, Y.-J. Kim, Y. Sinelnikov // Asia-Pacific Microwave Conf. Sydney, NSW, Australia, 3–6 Dec. 2000. P. 1187–1190. doi: 10.1109/APMC.2000.926043

25. Wideband Probe-Type Waveguide-to-Microstrip Transition for V-band Applications / O. Soykin, A. Artemenko, V. Ssorin, A. Mozharovskiy, R. Maslennikov // Proc. of 46th Europ. Microwave Conf. (EuMC). London, UK, 4–6 Oct. 2016. P. 1–4. doi: 10.1109/EuMC.2016.7824262

26. Shireen R., Shi S., Prather D. W. W-band microstrip-to-waveguide transition using via fences // Progress In Electromagnetics Research Lett. 2010. Vol. 16. P. 151–160.

27. A novel microstrip-to-waveguide transition using electromagnetic bandgap structures / Y. Tahara, A. Ohno, H. Oh-hashi, S. Makino, M. Ono, T. Ohba // Proc. of Intern. Symp. on Antennas and Propagation (ISAP), 2005. P. 459–462.

28. Pat. US 6 967 542 B2. Int. Cl. H01P 5/107; H01P 5/10; H01P 005/107 (2006.01). Microstrip-Waveguide Transition / M. E. Weinstein. Publ. 2005/11/22.

29. Пат. RU 2 600 506 C1. H01P 5/107 (2006.01). Волноводно-микрополосковый переход / О. В. Сойкин, В. Н. Ссорин, А. В. Можаровский, А. А. Артеменко, Р. О. Масленников; опубл. 20.10.2016. Бюл. 29.

## Информация об авторах

**Можаровский Андрей Викторович** – старший инженер по СВЧ-устройствам и антенной технике ООО "Радио Гигабит". Окончил Нижегородский государственный университет им. Н. И. Лобачевского (2011) по специальности "Информационные системы и технологии". Соискатель кафедры микрорадиоэлектроники и технологии радиоаппаратуры Санкт-Петербургского государственного электротехнического университета "ЛЭТИ" им. В. И. Ульянова (Ленина). Автор 30 печатных работ. Сфера научных интересов – антенно-фидерные устройства миллиметрового диапазона длин волн, включая печатные, волноводные и линзовые антенны и антенные решетки; планарные и волноводные дуплексирующие устройства и фильтры.
Адрес: ООО "Радио Гигабит", ул. Ошарская, д. 95, корп. 2, Нижний Новгород, 603105, Россия
E-mail: andrey.mozharovskiy@radiogigabit.com
https://orcid.org/0000-0002-9827-6720

**Сойкин Олег Валерьевич** – магистр радиофизических наук (2014), научный сотрудник ООО "Радио Гигабит". Исследователь. Преподаватель-исследователь (2018). Автор 13 научных публикаций. Сфера научных интересов – антенные системы для беспроводных систем связи; СВЧ-линии передачи/антенны и другие пассивные устройства; устройства миллиметрового диапазона длин волн.
Адрес: ООО "Радио Гигабит", ул. Ошарская, д. 95, корп. 2, Нижний Новгород, 603105, Россия
E-mail: oleg.soykin@radiogigabit.com

**Артеменко Алексей Андреевич** – кандидат технических наук (2013), директор по исследованиям и разработкам ООО "Радио Гигабит". Автор около 50 научных работ и 14 патентов. Сфера научных интересов – антенная техника, включая апертурные антенны, особенно антенны миллиметрового диапазона длин волн, антенные решетки, печатные антенны, антенны с электронным управлением лучом; СВЧ-техника, включая пассивные устройства и активные радиочастотные модули, такие, как волноводно-микрополосковые переходы, поляризационные селекторы, фильтры на металлических и поверхностных волноводах; СВЧ-приемопередатчики на современной электронной компонентной базе диапазонов частот от 0 до 90 ГГц.
Адрес: ООО "Радио Гигабит", ул. Ошарская, д. 95, корп. 2, Нижний Новгород, 603105, Россия
E-mail: alexey.artemenko@radiogigabit.com

**Масленников Роман Олегович** – кандидат физико-математических наук (2012), генеральный директор ООО "Радио Гигабит". Автор более 100 печатных научных работ и более 30 изобретений. Сфера научных интересов – алгоритмы оптимальной обработки сигналов в современных беспроводных системах связи.
Адрес: ООО "Радио Гигабит", ул. Ошарская, д. 95, корп. 2, Нижний Новгород, 603105, Россия
E-mail: roman.maslennikov@radiogigabit.com

**Вендик Ирина Борисовна** – доктор технических наук (1991), профессор (1993) кафедры микрорадиоэлектроники и технологии радиоаппаратуры Санкт-Петербургского государственного электротехнического

университета "ЛЭТИ" им. В. И. Ульянова (Ленина), руководитель лаборатории СВЧ-микроэлектроники названного университета. Член ряда международных сообществ, в том числе IEEE (senior member) и EuMA. Автор более 300 научных работ. Сфера научных интересов – исследование свойств материалов для электроники (сверхпроводники, сегнетоэлектрики, метаматериалы); разработка устройств микроволнового и терагерцового диапазонов.
Адрес: Санкт-Петербургский государственный электротехнический университет "ЛЭТИ" им. В. И. Ульянова (Ленина), ул. Профессора Попова, д. 5, Санкт-Петербург, 197376, Россия
E-mail: ibvendik@rambler.ru
https://orcid.org/0000-0001-5632-1223